

**DEUTERIUM-DEUTERIUM  
FUSION REACTIONS IN THE  
HOUGHTON COLLEGE  
CYCLOTRON**

By

Joshua Bowman

A thesis submitted in partial fulfillment of the  
requirements for the degree of

Bachelor of Science

Houghton College

May 2022

Signature of Author.....

Department of Physics  
May 12, 2022

.....

Dr. Mark Yuly  
Professor of Physics  
Research Supervisor

.....

Dr. Brandon Hoffman  
Professor of Physics

**DEUTERIUM-DEUTERIUM FUSION  
REACTIONS IN THE HOUGHTON COLLEGE  
CYCLOTRON**

By

Joshua Bowman

Submitted to the Department of Physics  
on May 12, 2022 in partial fulfillment of the  
requirement for the degree of  
Bachelor of Science

**Abstract**

The Houghton College Cyclotron is a miniature particle accelerator that uses two “dee” shaped hollow electrodes, of 15.6 cm radius, to accelerate ions across a gap with an alternating RF potential difference of a few thousand volts at a frequency of 5.831 MHz. As an ion accelerates, an up to 1.13 T magnetic field keeps it on a circular path that spirals outward, allowing the ion to accelerate multiple times using the same electric potential. In this experiment, deuterons were ionized by electrons from a filament and accelerated, with a current of about 20 nA and an approximate energy of 4.8 keV, into a copper target at a radius of 5.54 cm where they embedded themselves. Later deuterons striking the embedded deuterons caused the  $D(d,n)^3\text{He}$  reaction which produced neutrons. A plastic scintillator detector counted the neutrons that penetrated the chamber walls. An increase of  $7913 \pm 587$  counts or  $158 \pm 12$  counts per minute was detected when the beam was turned on. This is a significant milestone for the Houghton College Cyclotron as it is the first nuclear reaction that this cyclotron has successfully generated.

Thesis Supervisor: Dr. Mark Yuly  
Title: Professor of Physics

## TABLE OF CONTENTS

<b>Chapter 1: Introduction.....</b>	<b>6</b>
<b>1.1. Cyclotron Development.....</b>	<b>6</b>
<b>1.2 Small Cyclotrons .....</b>	<b>9</b>
1.2.1 The El Cerrito Cyclotron .....	10
1.2.2 Cyclotrino .....	10
1.2.3 Rutgers Cyclotron.....	10
1.2.4 Other small cyclotrons .....	10
<b>1.3 Houghton College Cyclotron .....</b>	<b>11</b>
1.3.1 Development.....	11
1.3.2 Performance .....	11
1.3.3 Problem of Phase.....	12
1.3.4 Motivation .....	12
<b>Chapter 2: Theory.....</b>	<b>15</b>
<b>2.1 Introduction .....</b>	<b>15</b>
<b>2.2 Fields.....</b>	<b>15</b>
<b>2.3 Phase.....</b>	<b>16</b>
<b>2.4 Radio Frequency Circuit.....</b>	<b>17</b>
<b>2.5 Focusing .....</b>	<b>18</b>
2.5.1 Electric Focusing.....	18
2.5.2 Weak Focusing.....	18
2.5.3 Strong Focusing.....	19
<b>2.6 Energy.....</b>	<b>20</b>
<b>2.7 Possible Reactions.....</b>	<b>21</b>
<b>Chapter 3: Experimental Apparatus .....</b>	<b>23</b>
<b>3.1 Overview.....</b>	<b>23</b>
<b>3.2 Gas Injection System.....</b>	<b>25</b>
<b>3.3 Chamber.....</b>	<b>25</b>
<b>3.4 Filament.....</b>	<b>26</b>
<b>3.5 Dees .....</b>	<b>27</b>
<b>3.6 RF Generation .....</b>	<b>27</b>
<b>3.7 Voltage Pickup .....</b>	<b>27</b>
<b>3.8 Magnet.....</b>	<b>28</b>
<b>3.9 Vacuum System .....</b>	<b>29</b>
<b>3.10 Target.....</b>	<b>29</b>
<b>3.11 Radiation Detector .....</b>	<b>30</b>
<b>3.12 Computer Control.....</b>	<b>31</b>
<b>Chapter 4: The D(d,n)<sup>3</sup>He Experiment .....</b>	<b>33</b>
<b>4.1 Overview.....</b>	<b>33</b>
<b>4.2 Experimental Procedure.....</b>	<b>33</b>
<b>4.3 Results .....</b>	<b>35</b>
<b>Chapter 5: Conclusion .....</b>	<b>36</b>

<b>Appendix A: LabVIEW Code.....</b>	<b>37</b>
<b>Appendix B: SMath Cross Section Calculation .....</b>	<b>39</b>

## TABLE OF FIGURES

Figure 1. An ion inside the acceleration chamber of a cyclotron.....	8
Figure 2. Proton trajectory in the cyclotron magnetic field as calculated by SIMION. ....	13
Figure 3. SIMION calculation of the vertical position versus radius. ....	13
Figure 4. A diagram depicting the forces on an ion accelerating in a cyclotron.....	16
Figure 5. The circuit used in the cyclotron to deliver RF power into the resonant LC circuit.....	18
Figure 6. Electric focusing between the dees of a cyclotron.....	19
Figure 7. Diagram depicting weak focusing.....	20
Figure 8. Measured cross sections for the $D(d,n)^3He$ reaction for energies of 0 to 100 keV. ....	22
Figure 9. Measured cross sections for the $D(d,n)^3He$ reaction for energies of 0 to 12 keV.....	22
Figure 10. The Houghton college cyclotron with its main systems labeled. ....	24
Figure 11. A block diagram for all the systems of the cyclotron, including computer control.....	24
Figure 12. A block diagram of the gas injection system of the Houghton College Cyclotron.....	25
Figure 13. The chamber of the Houghton College cyclotron. ....	26
Figure 14. The calibration circuit for the voltage pickup.....	28
Figure 15. The vacuum system of the Houghton College cyclotron.....	29
Figure 16. Mechanical drawings of the original target and new targets. ....	30
Figure 17. A block diagram of the circuit for the plastic scintillator detector.....	31
Figure 18. Measured beam current as a function of the magnetic field.....	34
Figure 19. Beam current as a function of magnet current near 255 mT. ....	35

## Chapter 1

### INTRODUCTION

#### 1.1. Cyclotron Development

In 1927, Ernest Rutherford, a professor at the University of Cambridge and the director of the Cavendish Laboratory, gave a speech [1] to the Royal Society in London. He addressed new advances in the generation of high voltages. Still, the millions of volts created by man were dwarfed by the voltages found in nature. He contended that these high potentials could be used to create high-energy ions, electrons, and electromagnetic radiation closer to the high energies created by natural processes, such as natural decay of radioactive isotopes. Rutherford wanted to see the resulting particles used to study disintegration of nuclei.

In the early 1920s, researchers only had primitive electrostatic accelerators to accelerate ions. These accelerators used enormous potentials of a few million volts applied across a single gap. Electrodes attached to a resistor divider were often placed in the gap to maintain a uniform electric field. Since the potential applied across the gap was so large, they were prone to arcing and corona discharges which would stop the accelerator from working properly. This problem made electrostatic accelerators unreliable and inefficient above energies of about 10 MeV.

To solve this problem, Gustav Ising proposed the radio frequency linear accelerator in 1925 [2], and Rolf Wideröe built the first working prototype in 1928 [3]. A linear accelerator consists of an ion source and a series of electrodes in a linear configuration. A high-voltage radio frequency is placed across a series of tube-shaped electrodes, such that adjacent electrodes have reverse polarity. As an ion travels between two electrodes, the electric field accelerates it until the ion passes through the far electrode. The radio frequency then swaps the polarity of the electrodes while the ion is in the field-free region inside the conducting hollow electrodes. Once the ion enters the gap between the next pair of electrodes, the ion is accelerated again. In Wideröe's accelerator, there were three electrodes in the series, giving ions an energy twice that of the accelerating potential. This accelerator allowed sodium and

potassium ions to be given energy up to about 100 keV for an accelerating voltage of 50kV. The great promise of this design was that linear accelerators could accelerate ions to high energies with a relatively low voltage, eliminating problems with arcing and corona discharges that plagued electrostatic accelerators.

In 1930, E. O. Lawrence, a professor of physics at the University of California, Berkeley, read Wideröe's paper in the university library [4]. He conceived of a new accelerator design, that would use the same voltage many times to accelerate particles along a circular path. This idea formed the basis for the first cyclotron [5]. In 1931, M. S. Livingston, a doctoral student working for Lawrence, built the first working prototype [6]. This accelerator was based on the same principles as the linear accelerator but used the same electric field multiple times to accelerate ions.

To accomplish this, inside the acceleration chamber of a cyclotron are two hollow, D-shaped electrodes called "dees," with a potential difference between them dependent on a radio frequency high voltage applied to the dees. An electromagnet creates a nearly uniform magnetic field inside the acceleration chamber. Ions start at the center and are accelerated toward one of the dees by the electric field until they pass into the dee. Then, while the ion is in the field-free region inside the conducting dee, the polarity of the electric field is swapped to accelerate the ion toward the other dee. This means that when the electric field is swapped, the particle is not affected by the change until it passes into the gap between the dees. As the particle moves, the magnetic field exerts a force perpendicular to the particle's motion so that it begins to orbit the center of the chamber as depicted in Figure 1. As the process repeats and the particle moves faster with each pass between the dees, the radius of the particle's orbit increases but the period of revolution remains the same. The constant period of revolution allows the same radio frequency to accelerate the ion through multiple passes. Livingston's first accelerator eventually achieved an energy of 80 keV for protons [6].

After the initial success of the cyclotron, further research went into perfecting the design. A much later paper [7] by Livingston in 1944 described a cyclotron at MIT that reached an energy of 16 MeV. Eventually, a critical limitation was discovered in the cyclotron. As particles approached the speed of light, they would fall out of phase with the radio frequency

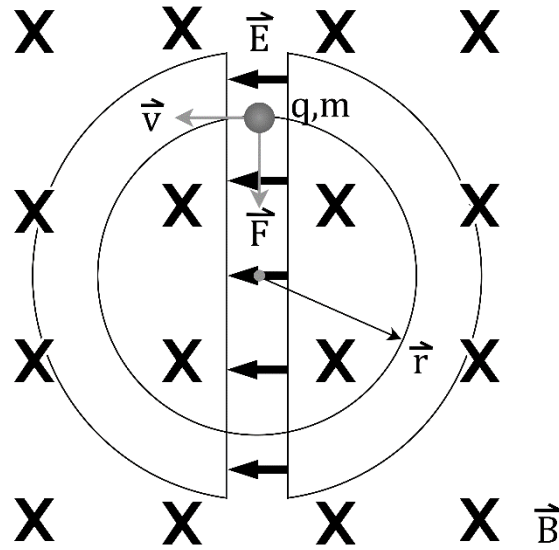


Figure 1. An ion with charge  $q$  and mass  $m$  inside the acceleration chamber of a cyclotron once it has reached a radius  $\vec{r}$ . The electric field between the dees,  $\vec{E}$ , exerts a force on the ion which accelerates the ion. As the ion gains velocity,  $\vec{v}$ , the magnetic field  $\vec{B}$  exerts a force on the ion,  $\vec{F}$ , perpendicular to its velocity. When the particle enters the dee toward which it is moving, the radio frequency will swap the direction of the electric field.

used for acceleration and decelerate without hitting a target. As the velocity of particles approaches the speed of light, the momentum of the ions increases quickly while their velocity increases slowly. This means that as the orbit radius increases, the period of revolution increases, changing the resonance frequency of the ions.

To overcome the limitations of the cyclotron, in 1945, E. M. McMillan, discoverer of neptunium and a leading researcher for the Manhattan Project, suggested using frequency modulation [8]. The radio frequency applied across the dees would be changed as the particles approached relativistic speeds to account for relativistic effects. This is the foundational principle for the synchrocyclotron. A synchrocyclotron, or frequency-modulated cyclotron, is a cyclotron in which the frequency applied across the dees changes cyclically to produce bursts of relativistic ions. Based on this principle, the 184-in. cyclotron magnet, conceived by Lawrence and brought to the Manhattan District for other uses during World War II, was converted into a synchrocyclotron [9]. Although synchrocyclotrons succeeded in creating relativistic particles for study, they have a major deficiency. Since they produce pulses of particles, the effective beam current is only around 1% that of a cyclotron.

These have generally been phased out in favor of synchrotrons which are more cost-effective. A synchrotron uses a series of magnets, placed along a ring, that increase in field strength as the particles accelerate, keeping particles accelerating at a constant orbit radius. This series of smaller magnets provides a magnetic field to curve the path of the particles without the use of a large central magnet, helping make synchrotrons cheaper than synchrocyclotrons. The electric field used to accelerate the particles is applied by multiple gaps, like the dees of a cyclotron, placed along the path of the particles. The potential difference applied across the gap must also change over time to account for the changing orbit period. Synchrotrons allow for far greater energies than synchrocyclotrons, extending into the TeV range.

Today, most cyclotrons are small and used for industrial and medical applications, since their small size and lower energy output makes them less useful in higher energy research than synchrotrons. In healthcare, cyclotrons are used to produce positron emitters for PET scans and radioactive isotopes to aid in imaging tumors [10]. In industry, cyclotrons can be used to activate a part of a machine to determine wear or to simulate neutron radiation damage [10]. Their compact form, lower operating costs, and relatively high ion energies make them ideal for these applications. They are also useful for low energy nuclear physics research, as they can accelerate particles and direct them into a target to create low energy nuclear reactions. Small cyclotrons can be used to generate neutrons, cause deuterium-deuterium fusion, and allow observation of many other reactions. Even today, a few large research cyclotrons are still operational. One is the largest cyclotron in the world, at TRIUMF in Canada, that can create up to 520 MeV protons [11]. The National Superconducting Cyclotron Lab in Michigan uses its cyclotrons to generate beams of rare isotopes [12] for research.

## **1.2 Small Cyclotrons**

Industry and advanced research laboratories are not the only entities to build and operate cyclotrons. Despite the high costs of building particle accelerators many individuals and groups have also built cyclotrons. Due to the cost, these cyclotrons are generally small and somewhat unrefined but can still be used for nuclear research.

### *1.2.1 The El Cerrito Cyclotron*

In 1947, four students at El Cerrito High School built a cyclotron [13], the twenty-fifth in the United States. This was significant in that they managed, for only \$600, to build a piece of equipment that, at the time, generally cost tens of thousands of dollars. This cyclotron had a diameter of six inches and could successfully accelerate ions. They eventually claimed to produce protons with energies around 1 MeV. It attracted international attention, as professors and students were inspired by how much young, determined physicists could accomplish.

### *1.2.2 Cyclotrino*

In 1981, a cyclotron to be used as a high-resolution mass spectrometer was constructed at the University of Berkely in California [14]. It utilized a 12-inch magnet, producing a magnetic field of about 1 T. It was able to produce a beam with an energy of about 40 keV, but its purpose was to detect carbon-14 for carbon dating, separating the particles by their mass. Due to the large number of orbits, the mass resolution was very good, allowing it to separate unwanted isotopes with nearly the same mass. Although not as effective for use in radiocarbon dating as originally hoped, it did show promise in detecting carbon-14 for biomedical applications.

### *1.2.3 Rutgers Cyclotron*

In 1995, Rutgers undergraduate Timothy Koeth decided he wanted to build a cyclotron at Rutgers University [15]. Originally, this cyclotron used a 9-inch magnet that allowed for energies of up to 600 keV for protons. A beam at this energy was first obtained in 1999. Later, the magnet was upgraded to a 12-inch magnet that first produced a beam in 2001. This cyclotron cost about \$15,000 due to recycling of parts but could have cost as much as \$250,000 if built using new parts. This cyclotron was used primarily for teaching in lab classes.

### *1.2.4 Other small cyclotrons*

There are many other recent examples of small cyclotrons being built for research and educational purposes. In 2007, a small cyclotron was built at MIT that could accelerate protons to 2 MeV [16]. As of 2009, two teenagers, Heidi Baumgartner and Peter Heuer, had

built a small cyclotron [17] capable of accelerating protons to 2.4 MeV at Jefferson Lab. It was eventually moved to Old Dominion University for continued development as a student project. As of 2013, a small cyclotron called Columbus, expected to produce protons with energies of 24 to 48 keV, was being constructed in Germany [18] as a prototype low-cost cyclotron for educational uses. In 2020, Martin Prechtel and Christian Wolf published a book [19] to aid in construction of small accelerators for educational purposes, using the Columbus cyclotron as a teaching example.

### **1.3 Houghton College Cyclotron**

Over the years, Houghton College has been building its own small cyclotron for research. The design of the cyclotron has undergone many changes during its development. Although its efficacy is somewhat limited by problems with focusing and phase, the cyclotron is finally capable of producing nuclear reactions for research.

#### *1.3.1 Development*

Since the original designs for the Houghton college cyclotron, many important systems have changed. The first designs had brass chamber walls and dees with aluminum chamber lids placed between the poles of a 0.5 T permanent magnet [20]. It had a theoretical maximum energy for protons of 45–170 keV. By 2006, a 1.1 T electromagnet had been adopted [21] and the dees were made from copper rather than brass. The theoretical maximum energy for deuterons increased from 18.7 keV to 150 keV. In 2007, arcing in the chamber damaged the dee and insulation [22]. By 2009, new chamber was constructed from aluminum in which the flanges were connected to the chamber wall using vacuum epoxy, which proved unreliable and prone to leak. Still, protons, hydrogen, and helium had been successfully accelerated by the cyclotron [22]. In her 2015 thesis, Sylvia Morrow explained that a new aluminum chamber had been machined with welded flanges to reduce leakage and discussed focusing problems in the cyclotron [23].

#### *1.3.2 Performance*

The Houghton College Cyclotron is a 1.13 T miniature cyclotron with a theoretical maximum energy of 400 keV for protons [24] with weak focusing. Despite this theoretical maximum,

the cyclotron has only been able to accelerate protons to 160 keV, as this estimate fails to consider that with weak focusing, ions fall out of phase.

### *1.3.3 Problem of Phase*

In her senior thesis, Sylvia Morrow addressed the problem of phase [23]. In the Houghton College Cyclotron, the magnetic field is not perfectly uniform, this difference becoming more pronounced toward the edges. As the magnetic field becomes weaker, the frequency required to accelerate the ions changes. As the required frequency changes, the ions fall increasingly out of phase with the frequency. For ions accelerating to higher energies, which must travel many times around the chamber while accelerating, this effect is more pronounced. Eventually, the ions will enter the gap between the dees early enough that they experience a net deceleration by the electric field. Thus, the ions spiral back to the center of the chamber and fail to hit the target. This limits the maximum energy to which the cyclotron can accelerate ions. Morrow simulated this phenomenon using SIMION 8.1 and Poisson Superfish. Figure 2 shows the path of an accelerating ion, never reaching the maximum possible radius as it falls out of phase and spirals back to the center of the chamber. and Figure 3 shows that, although weak focusing causes problems with phase, it is beneficial and necessary to keep the ions focused in the central plane of the chamber. To counteract the effect of the weakening of the magnetic field, future work will be done exploring strong focusing by creating sector pole tips that will make an azimuthally varying magnetic field that will focus the beam into the center of the center of height of the chamber while also maintaining a constant accelerating frequency over the entire radius of the cyclotron chamber. With strong focusing, the theoretical maximum energy would increase to 900 keV.

### *1.3.4 Motivation*

Many motivating factors lie behind the creation and continued operation of the Houghton College Cyclotron. One motivating factor is the many experiments that can be conducted using even small cyclotrons. Specifically, this cyclotron can cause low-energy nuclear reactions. One example is deuterium-deuterium fusion, which produces approximately 2.45 MeV neutrons. These neutrons can be used to activate materials using the  $(n,\gamma)$ ,  $(n,2n)$ , and

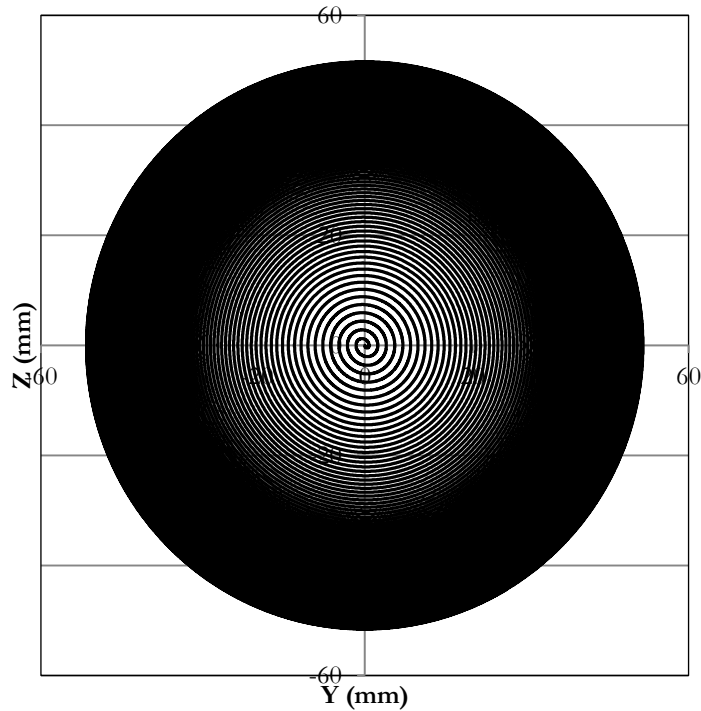


Figure 2. The proton trajectory in the cyclotron magnetic field as calculated by SIMION. This simulation was conducted with an RF voltage of -1500 V, or 3000V peak to peak, and a resonance frequency of 19.34 MHz. The maximum radius for protons is 51.5 mm, far short of the 79 mm maximum dee radius, as the proton falls out of phase and spirals back toward the center. This diagram was taken from Ref. [23].

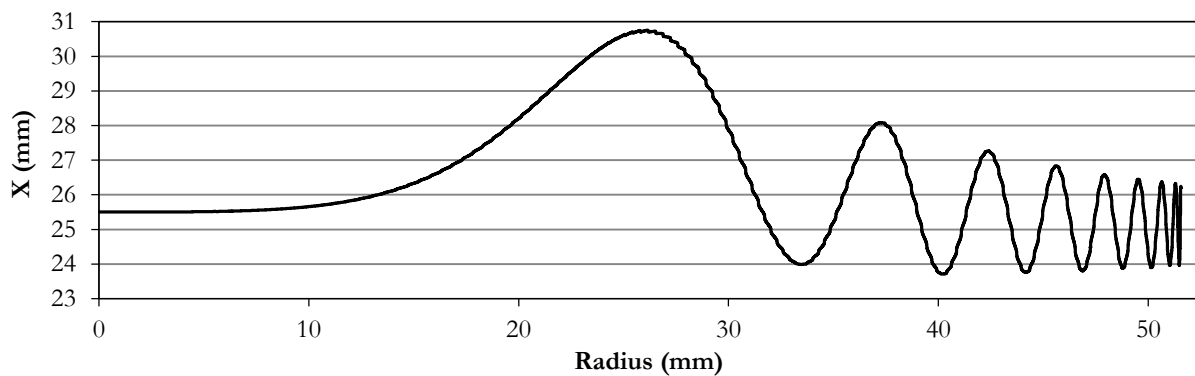


Figure 3. SIMION calculation of the vertical position versus radius for the cyclotron magnet. This simulation was conducted with an RF voltage of -1500 V, or 3000V peak to peak, and a resonance frequency of 19.34 MHz. The ion starts in the central plane of the chamber, at  $X = 25.5$  mm, with no kinetic energy, then oscillates in the axial direction around the central Y-Z plane. The amplitude of oscillation changes inversely with radius due to weak magnetic focusing of the particles. This diagram was taken from Ref. [23].

(n,p) reactions. In the case of (n, $\gamma$ ) and (n,2n), the outgoing gamma ray and neutrons can penetrate the chamber wall and be detected outside the cyclotron, allowing the use of an internal target. Some examples are the  $^{19}\text{F}(p,\alpha\gamma)^{16}\text{O}$  resonances at 224, 340, and 484 keV, the  $^{31}\text{P}(p,\gamma)$  resonances at 355, 440, and 540 keV, and the  $\text{D}(d,n)^3\text{He}$  reaction. Moreover, the design of a cyclotron is an interesting research problem, since phase and focusing are problems faced by all cyclic particle accelerators.

## Chapter 2

### THEORY

#### 2.1 Introduction

Although cyclotrons are very complex machines, the basic theory is relatively simple. The resonance frequency and energy follow directly from the forces on the particle and its motion through the chamber. The maximum energy is very important because it determines which nuclear reactions are achievable in the accelerator. A major difficulty in many cyclotrons is focusing. Achieving good focusing is difficult while maintaining an optimal phase relationship.

#### 2.2 Fields

The motion of an ion in a cyclotron can be explained by the electric and magnetic fields exerting forces upon it. Inside the chamber of a cyclotron are two hollow, D-shaped electrodes called “dees,” as shown in Figure 1. These electrodes are connected to a radio frequency voltage source that creates an electric field between the electrodes. A low-pressure gas fills the chamber where a filament, located at the center, bombards the molecules with electrons, which ionize them by removing the electrons from the gas molecules. Air must be evacuated from the chamber to decrease ion collisions with air molecules as the ions accelerate. The positively charged ions are accelerated by electric and magnetic fields. The electric field between the dees gives the ion a kick each time it enters the gap between the dees. As the ion moves, a magnetic field exerts a force perpendicular to the ion’s velocity. This force points toward the center of the chamber and curves the ion’s path into a circle. When the ion crosses the gap and enters the opposite dee, the radio frequency causes the charge of the dees to swap. Inside a conductor, such as either dee, the electric field is zero, so the ion is not affected by this change until it reaches the gap between the dees. The ion is then accelerated toward the other dee. The force on these ions is:

$$\vec{F} = \vec{F}_E + \vec{F}_B = q\vec{E} + q(\vec{v} \times \vec{B}) = m \frac{d\vec{v}}{dt} \quad (1)$$

where  $\vec{F}_E$  is the force on the ion due to the electric field and  $\vec{F}_B$  is the force on the ion due to the magnetic field as shown in Figure 4. Between the dees, the ion of charge  $q$  and mass  $m$  is in an electric field  $\vec{E}$ . The ion has velocity  $\vec{v}$  and is in magnetic field  $\vec{B}$ . This differential equation can be solved to give the path of the ion as it moves in the chamber.

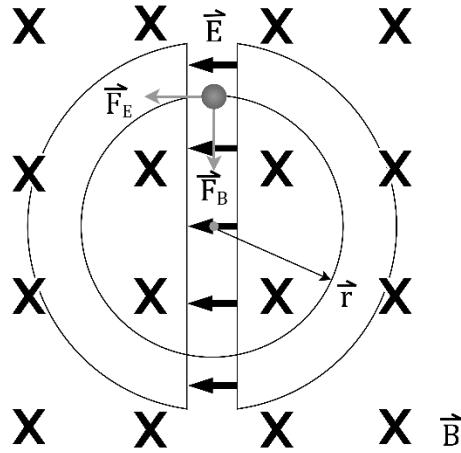


Figure 4. A diagram depicting the forces on an ion accelerating in a cyclotron.

### 2.3 Phase

When not between the dees, the ions move in a circle. The electric field between the dees must therefore oscillate with a radio frequency so that the ions are accelerated by the electric field when they are in the gap between the dees. The orbit of the ions must be in phase with the cyclotron dee voltage oscillation to experience optimal acceleration by the applied radio frequency.

The derivation below follows that given by Livingston and Blewett [4]. For a given ion with velocity  $v$ , the central force required to travel in a circular path of radius  $r$  is supplied by the Lorentz force:

$$\vec{F} = -\frac{mv^2}{r}(-\hat{r}) = q\vec{v} \times \vec{B}. \quad (2)$$

Solving this for  $v$  yields:

$$v = \frac{qBr}{m} \quad (3)$$

since  $\vec{v}$  and  $\vec{B}$  are perpendicular. The frequency of revolution,  $f$ , can be found by dividing the velocity by the distance travelled in an orbit, the circumference of the orbit:

$$f = \frac{v}{2\pi r} = \frac{qB}{2\pi m}. \quad (4)$$

In a constant magnetic field and under non-relativistic conditions, the frequency is constant as the ion accelerates. The particles may also be accelerated using this frequency multiplied by an odd number. This causes the polarity of the dees to switch multiple times while the ion is inside one of the dees, but the polarity of the dees is correct for accelerating the ion once it reaches the dee gap. Thus, this has no effect on acceleration. The selected resonance frequency is an odd integer multiple of other frequencies, so these lower frequencies can have resonance peaks corresponding lower magnetic fields that, while usable, would accelerate ions to significantly lower energies.

## 2.4 Radio Frequency Circuit

The frequency applied to the dees is produced by a resonant LC circuit. The dees and chamber of the cyclotron have a capacitance between them. By adding an inductor to this circuit, a resonant LC circuit is created. The resonance frequency of this circuit is:

$$f = \frac{1}{\sqrt{LC}} \quad (5)$$

where  $L$  is the inductance of the inductor and  $C$  is the capacitance of the capacitor, as shown in Figure 5. To deliver power to the LC circuit the RF power circuit is magnetically coupled to the circuit using another inductor. The magnetic flux through this inductor is coupled by mutual inductance to the inductor in the LC circuit so that the magnetic field created in the powered inductor induces a voltage in the LC circuit. This setup is advantageous because it allows for a large potential difference between the dees with a relatively small RF signal.

The input impedance must be tuned to ensure that it matches the output impedance of the RF amplifier so that power is delivered to the LC circuit without being reflected. This is done by inserting capacitors or inductors into the RF power circuit, which can be done automatically by an antenna tuner.

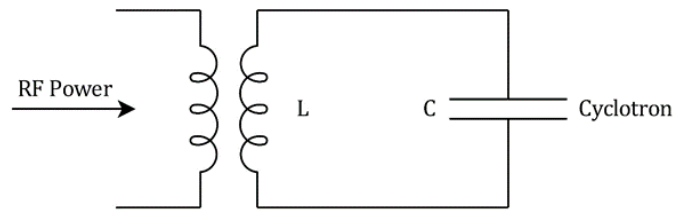


Figure 5. The circuit used in the cyclotron to deliver RF power into the resonant LC circuit.

## 2.5 Focusing

Until now, the motion of particles in a cyclotron has been modeled in two dimensions, confined to the central plane of the chamber. If particles have velocity perpendicular to this plane, they may hit the top or bottom of the chamber before they reach their target. Multiple techniques may be employed to ensure particles stay in the central plane.

### 2.5.1 Electric Focusing

Electric focusing occurs between the dees of a cyclotron's accelerating chamber. As shown in Figure 6, the geometry results in a nonuniform electric field between the dees through which particles must pass if they do not stay in the central plane of the chamber. This electric field pushes the ions toward the center as of the gap as they move through the first half of the distance between the dees, then pulls the particles away from the center as they pass through the second half of the gap. Since the ions accelerate through the gap, they spend less time in the portion that causes them to diverge, resulting in a net focusing effect. As the electrons move faster, the difference in time becomes insignificant, so this effect becomes negligible at higher energy, and therefore larger radii.

### 2.5.2 Weak Focusing

Weak focusing is produced by a magnetic field that decreases radially in the cyclotron. In this case, there is a component of the magnetic force that returns ions back to the central plane, as shown in Figure 7. The magnetic force can act, to a small degree, in the vertical direction since the field is not perfectly vertical. For this to happen, shims are usually placed between

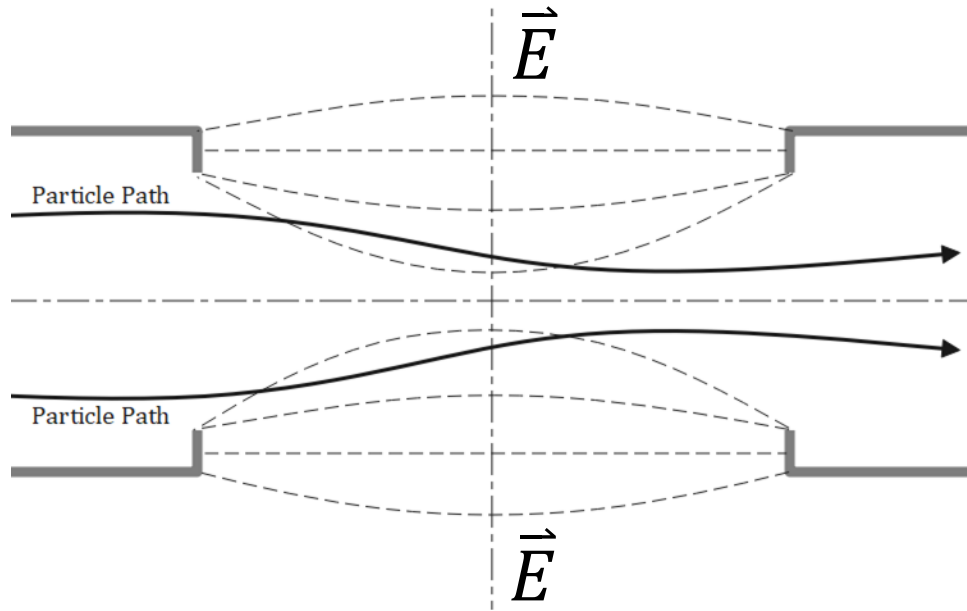


Figure 6. Electric focusing between the dees of a cyclotron. The non-uniform electric fields and acceleration of the particles cause a lens-like effect that results in net focusing. This figure was adapted from Ref. [4].

the magnets and the accelerating chamber to create the desired field shape. Unfortunately, the decreased magnetic field is no longer suitable for maintaining the correct resonance frequency. The ions will fall more and more out of phase with the oscillating electric field until they eventually reach  $180^\circ$  out of phase and are decelerated by the field, spiraling back to the center of the chamber. The acceptable rate of decrease is proportional to the dee voltage varies inversely with the final energy of accelerated ions. Less powerful cyclotrons use a weak magnetic field or high dee voltages so that ions require very few orbits to reach their final energy. Thus, cyclotrons that reach lower energies are less easily affected by radial changes in their magnetic field. A typical low-energy cyclotron can have a radial magnetic field decrease as high as four percent and a high-energy cyclotron should have a much smaller radial magnetic field decrease of about one percent [4].

### 2.5.3 Strong Focusing

One solution to the problems caused by weak focusing is strong focusing. Strong focusing keeps the average magnetic field the same by varying the field with angle using sector pole tips. Since the average magnetic field is constant, the time for an ion to orbit the chamber remains the same. Thus, the frequency is constant. Once the field is shaped with angle, the

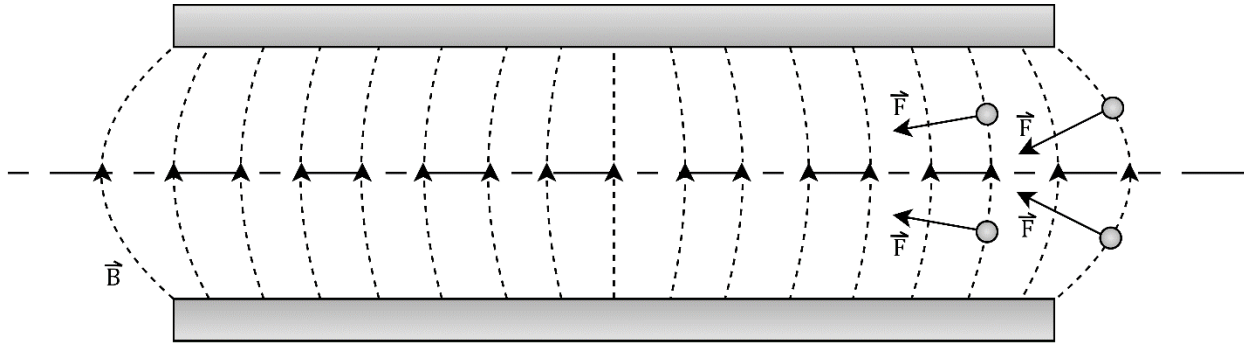


Figure 7. Diagram depicting weak focusing. This diagram was adapted from Ref. [4].

accelerating ion experiences regions of increasing and decreasing field as it orbits, which provide focusing in much the same way as weak focusing.

## 2.6 Energy

The amount of energy gained by a particle on each pass between the dees is:

$$\Delta T = q\phi \quad (6)$$

where  $T$  is the kinetic energy of the particle,  $q$  is the charge on the particle, and  $\phi$  is the change in potential across the dees. This energy is generally written in the units of electron-volts, or eV where one electron-volt is equal to  $1.602 \times 10^{-19}$  J. The number of orbits an ion makes before it reaches the target can also be calculated:

$$T = 2N\phi e \quad (7)$$

where  $N$  is the number of full revolutions the ion has made. The kinetic energy of an accelerating ion is:

$$T = \frac{1}{2}mv^2 = \frac{1}{2}\frac{q^2}{m}B^2R^2 \quad (8)$$

using the velocity from Equation (3).

This equation can be used to calculate the energy of ions incident on a target using the target radius. It also shows that the kinetic energy of an ion increases like the square of the magnetic field strength and the final radius of the ion before it strikes the target.

## 2.7 Possible Reactions

All nuclear reactions have a cross section, which is proportional to the likelihood that a reaction will occur. In nearly all reactions at very low energy, the likelihood increases as the energy of the incident particle increases, but most also have a minimum required energy, or threshold, for any reactions to take place, as shown in Figure 8 and Figure 9. As a small cyclotron can only accelerate protons to at most a few MeV and other ions far less, depending on charge and mass, many reactions cannot be attempted. Still, there are also many reactions, such as deuterium-deuterium fusion that can occur in the 100 keV range. Deuterium-deuterium fusion also generates a 2.45 MeV neutron that may be used to facilitate other reactions, perhaps even higher energy reactions than could be created by the accelerator's beam.

The number of reactions that occur in a period of time can be estimated to determine if an experiment is viable. To cause the  $D(d,n)^3\text{He}$  reaction, deuterons are accelerated into a copper target and many stick to the target. Later deuterons strike embedded deuterons, causing fusion. A reasonable estimate can be obtained, as shown in Appendix B, by first estimating the number of target nuclei embedded in the copper:

$$N = \frac{i \cdot t}{e} \quad (9)$$

where  $i$  is the beam current,  $t$  is time, and  $e$  is the charge on an electron. Then, the number of reactions that occur after  $N$  atoms are embedded can be estimated. This is proportional to the cross section, beam current, number of embedded deuterons, and time. It must be inversely proportional to the beam area and charge on an electron. This, the number of reactions must be proportional to:

$$Y = \sigma \frac{i N}{e A} t \quad (10)$$

where  $\sigma$  is the cross section of the reaction and  $A$  is the area of the beam spot. This estimate assumes that after the detector starts counting, no more deuterons will embed in the copper. This estimate predicted that 2.2416 reactions would occur per hour. This value is highly dependent on the cross section used, which is not certain, as shown by the conflicting data in Figure 9. In reality, the actual number of reactions could be much higher or lower.

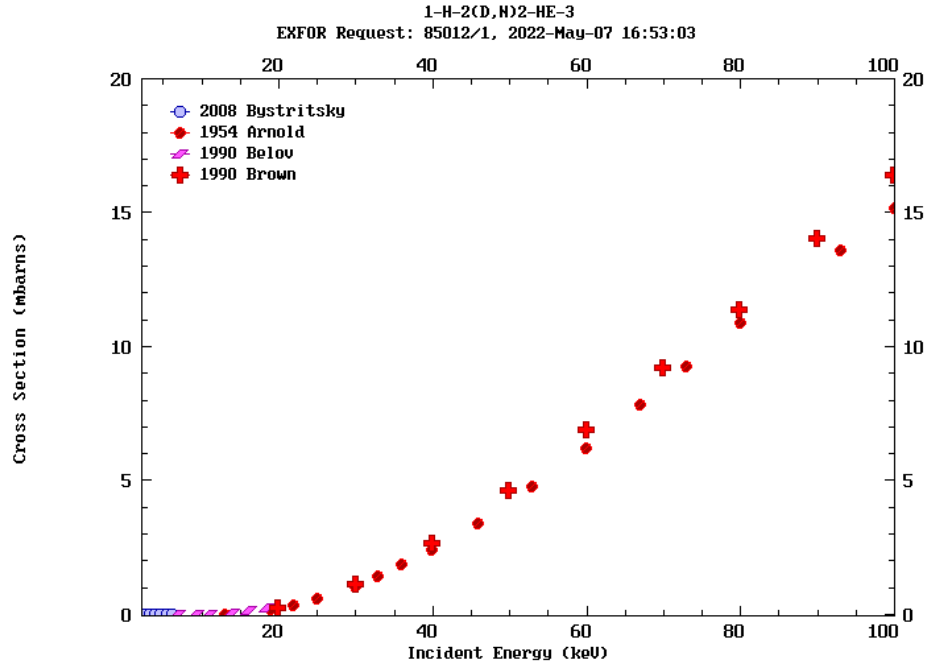


Figure 8. Measured cross sections for the  $D(d,n)^3\text{He}$  reaction for energies of 0 to 100 keV. This plot was taken from Ref. [25] with data from Ref. [26].

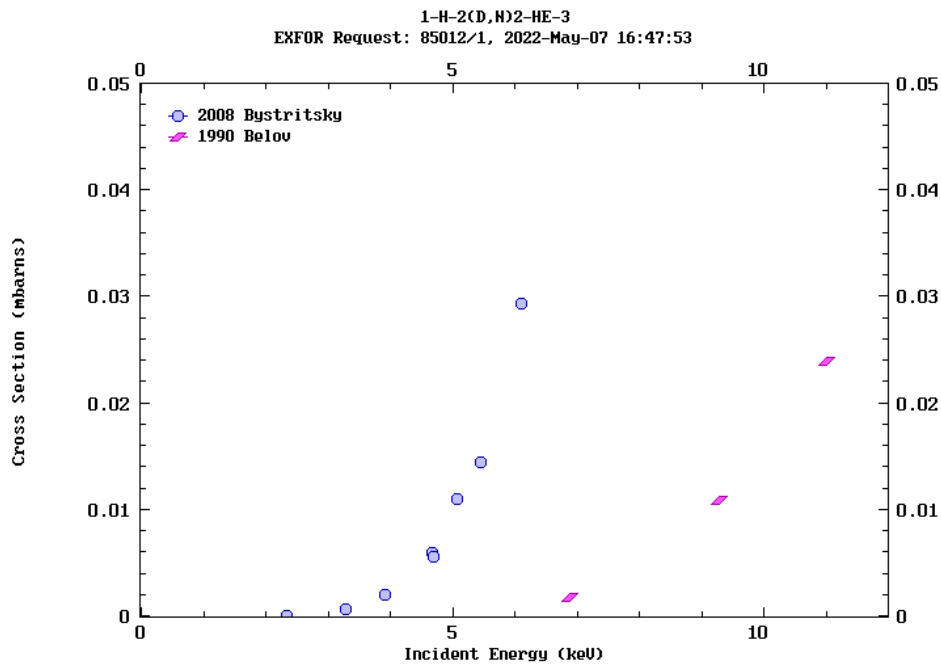


Figure 9. Measured cross sections for the  $D(d,n)^3\text{He}$  reaction for energies of 0 to 12 keV, allowing for closer examination of data. This graph was taken from Ref. [25] with data from [26].

## Chapter 3

### EXPERIMENTAL APPARATUS

#### 3.1 Overview

This chapter describes the six main systems of the cyclotron, as well as the detector used to detect nuclear reactions. These systems are shown in Figure 10 except for the gas injection system, which is behind the cyclotron, and Figure 11 shows the block diagram for all the electronics in the cyclotron. Gases to be accelerated are stored under pressure in a cylinder and allowed to enter the chamber through the very slow leak created by a needle valve. In the center of the vacuum chamber is the filament, which is composed of a tungsten wire that, when powered, ejects electrons by thermionic emission. These electrons knock electrons off gas molecules, creating ions that can be accelerated by electric and magnetic fields. The necessary electric field is created by a hollow, D-shaped, aluminum electrode called a “dee” and a grounded “dummy dee”. As they accelerate, they may sometimes collide with air or gas particles in the chamber. To minimize this problem, the air is removed from the chamber by vacuum pumps. A magnet is used to curve the trajectories of the ions into circles so that they can be accelerated multiple times by the same potential. A high voltage radio frequency is applied to the dees so that the ions experience an accelerating electric field on each pass between the dees. This signal is generated using mutual inductance to an LC circuit. Inside the chamber, very close to the dee, is a voltage pickup that is used to monitor the dee voltage. As the ions accelerate, they spiral outward, eventually reaching the radius of the target, which they will strike. This target can be used to create nuclear reactions or, with an attached electrometer, to monitor the beam current. A radiation detector placed outside the chamber can detect the products of nuclear reactions that occur to verify that a reaction is occurring. Many of the systems of the cyclotron are computer-controlled, increasing safety and allowing automation.

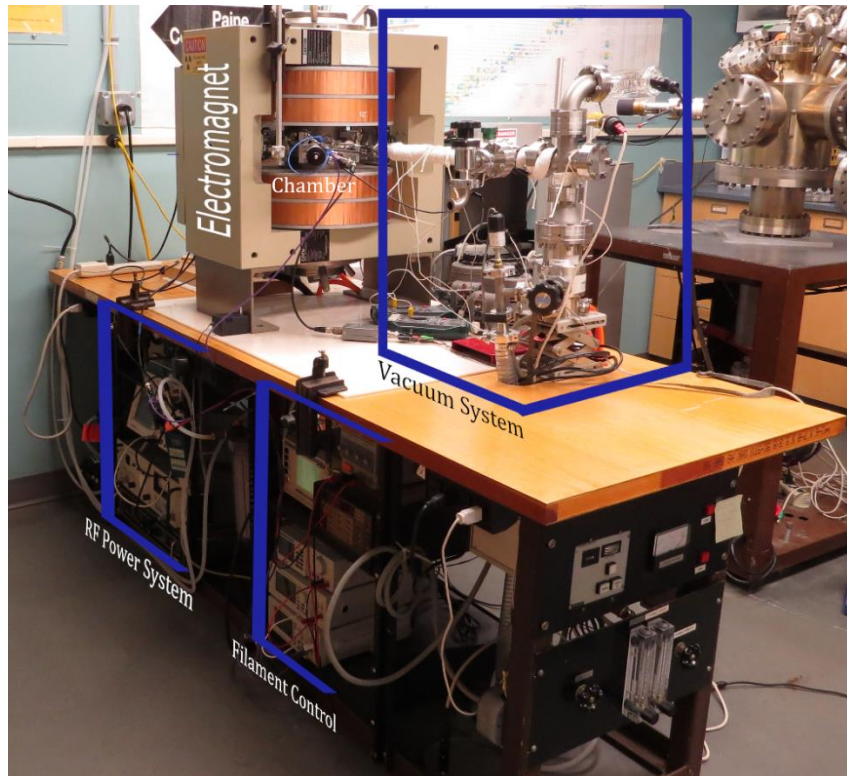


Figure 10. A photograph of the Houghton college cyclotron with its main systems labeled.

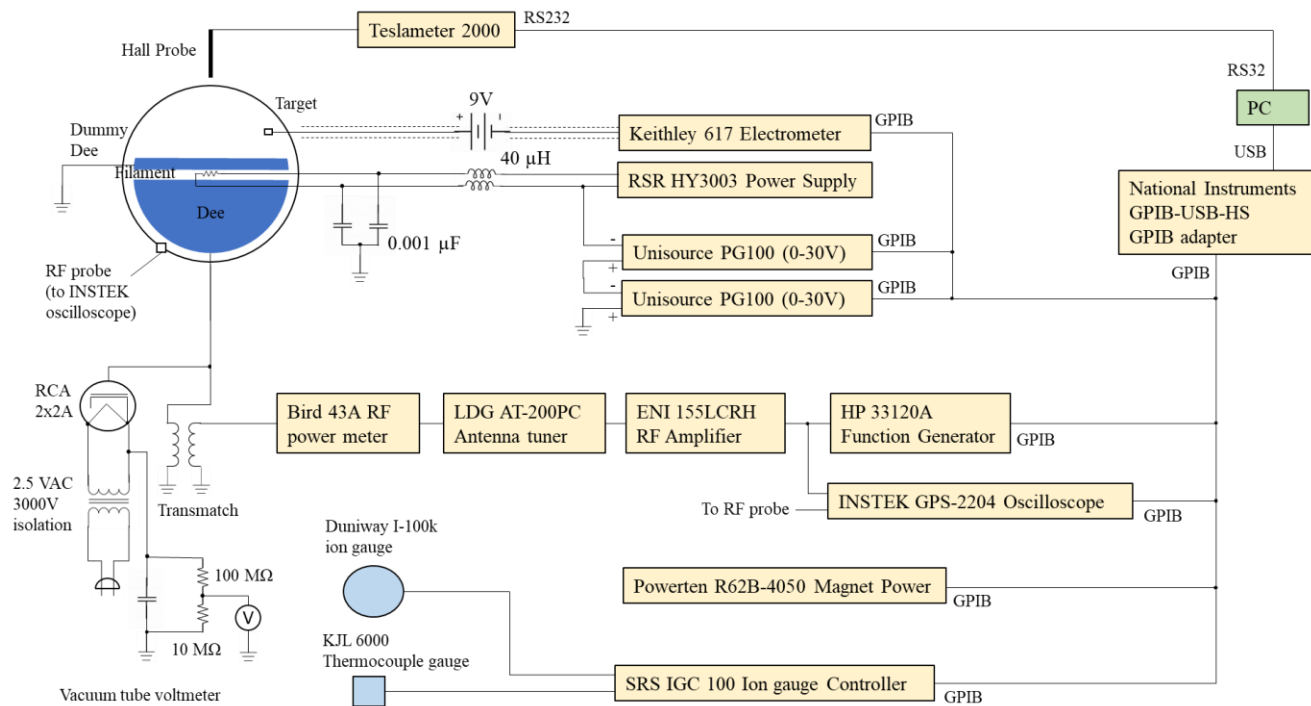


Figure 11. A block diagram for all the systems of the cyclotron, including computer control.

### 3.2 Gas Injection System

The gas to be injected into the cyclotron is stored in a pressurized cylinder, which is connected by vacuum connections to an Edwards LV10K needle valve, which is attached to the chamber of the cyclotron via a BOC Edwards SP16K valve. To allow gas into the chamber, the cylinder is opened, and the regulator is set to a pressure slightly above atmospheric pressure. The valve to flush is opened for up to a minute to remove air from the system up to the needle valve. This valve is closed and the valve to the chamber is opened, removing the air from the system past the needle valve. Next, needle valve is opened slowly until the pressure in the chamber, read off the RGA, raises very slightly. If the pressure is too high, the needle valve is closed, and slightly opened until the desired pressure is obtained inside the chamber.

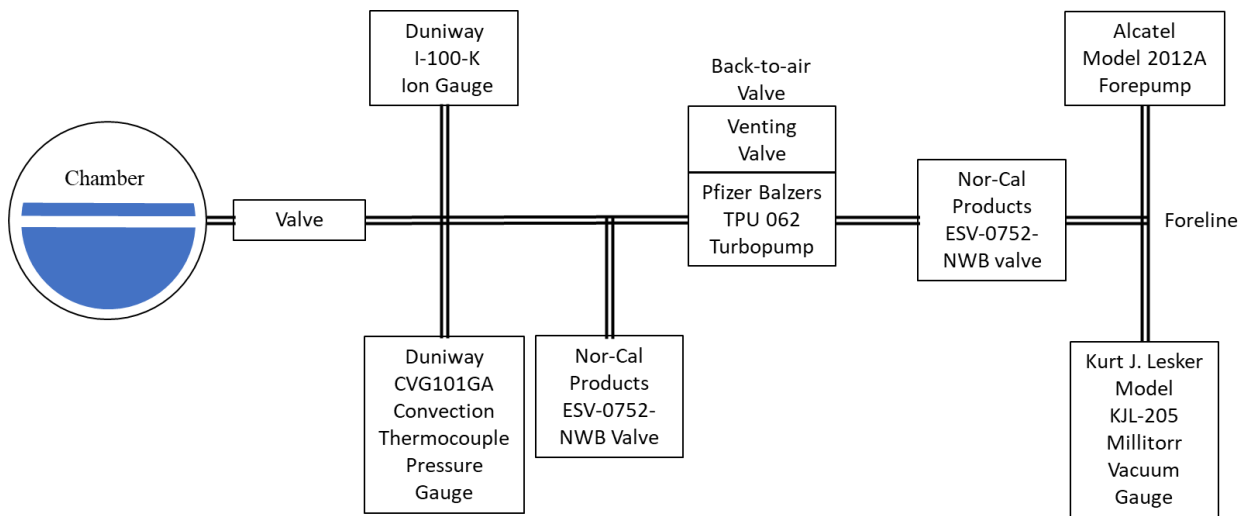


Figure 12. A block diagram depicting the gas injection system of the Houghton College Cyclotron.

### 3.3 Chamber

The vacuum chamber consists of a ring of aluminum 2.6 cm tall with an inner diameter of 8.75 cm and an outer diameter of 9.8 cm. Above and below this ring are two lids, each sealed by a 262 Viton O-ring. The lids and ring are held securely together by 5 clamps around the diameter of the chamber. Evenly spaced around the ring are ten QF 16 flanges that are welded to the ring to ensure an air-tight seal. Passing through these flanges are the two ground wires for the dummy dee, the target holder, the RF voltage pickup, the RF dee stem,

power for the filament, a window, a connection to the vacuum pumps, and a connection to allow gas to enter the chamber.

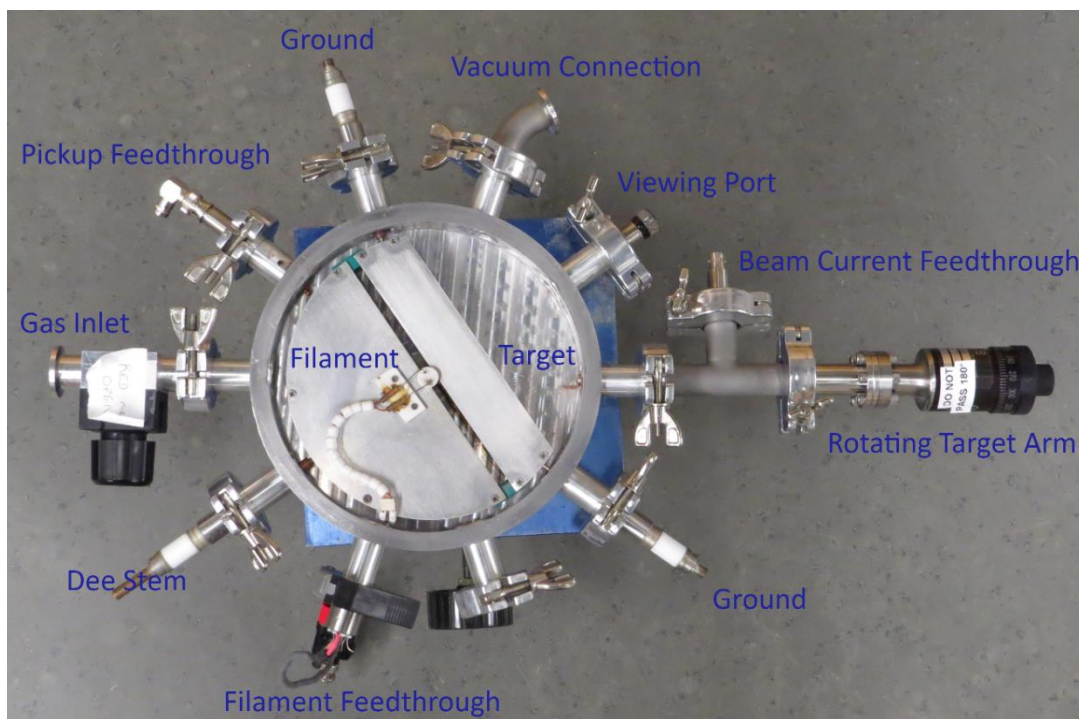


Figure 13. A photograph of the chamber of the Houghton College cyclotron. The main components and ports are labeled.

### 3.4 Filament

Inside the chamber, the gas molecules are ionized by electrons from the filament, which is positioned on top of the dees in the center of the vacuum chamber. The filament is composed of a 0.05 mm diameter thoriated tungsten wire, bent into a hairpin shape, running between two electrodes spaced at 6.45 mm. The filament is controlled by three power sources: two P6100 programmable power supplies that keep the filament floating at -60 V and an RSR HY3003 DC power supply that supplies a current of up to about 2 A through the filament. Since the filament floats at a negative potential as it is heated by the current, it ejects electrons which are also supplied by the 1.9 A current. The wires that travel over the dee are separated by ceramic spacers to prevent shorting. Since a high voltage radio frequency is applied to the dees very near to the filament, this RF can be picked up by the filament leads and result in damage to the power supplies. To prevent this, an RF filter was placed between

the filament and power supplies. This consists of a capacitor that shorts radio frequencies to ground and an inductor that resists changes in current flowing from the power supplies.

### **3.5 Dees**

Housed in the chamber, the dees are spaced 1.1 cm apart and held at a fixed distance by two 3D printed plastic spacers. The outer diameter of the dees is 15.6 cm. The larger dee is connected to the radio frequency circuit by the dee stem, while the dummy dee is grounded. This setup is easier to create than two dees, oscillating in opposite phase and means that the accelerating voltage is equal to the radio frequency voltage.

### **3.6 RF Generation**

The RF signal applied to the dees originates in a Hewlett Packard 33120A function/arbitrary waveform generator. The function generator was set to output a sine wave at the resonance frequency. This signal was then amplified by a Kalmus model 155LCRH RF power amplifier with a maximum power output of 100 W and a frequency range of 0.1 to 10MHz, which is the limiter for usable signal frequency values. This power amplifier has a built-in meter that displays the power output, but a Bird Electronic Corp. Wattmeter with a 250 W, 2 to 30 MHz element was used to ensure accurate readings. To determine the resonant frequency, a capacitance and inductance meter was used to measure the capacitance of the dee and chamber wall. The inductance of the inductor was also measured, then these values were used to calculate the approximate frequency of the LC circuit. Next, a NanoVNA was attached to determine the precise resonance frequency of the LC circuit. The frequency for minimum voltage standing wave ratio (VSWR) was found, which is where the power entering the circuit is reflected least. This frequency, 5.831 MHz, was the resonance frequency of the cyclotron and was entered into the function generator. The LDG Electronics AT-200PC antenna tuner was then connected to the LC circuit. This device automatically inserts capacitors and inductors to match the impedance of the RF power circuit to that LC circuit to ensure optimal efficiency. It can also be used to measure the RF power.

### **3.7 Voltage Pickup**

A few millimeters from the top of the larger dee is a small coil of copper wire in which a current is induced when the electric field of the dee changes. The resulting measured voltage

depends on the input impedance of the scope and is proportional to the voltage on the dee. This allows for monitoring of the accelerating voltage through a GW Instek GDS-2204 digital oscilloscope to ensure the desired potential is achieved between the dees. It is especially important to ensure the voltage of the dees does not surpass 3000 V peak-to-peak which, in the past, resulted in arcing and damaged the filament insulator and dee.

To determine the exact voltage on the dees, the voltage pickup was calibrated. To that end, a circuit, depicted in Figure 14, was connected that rectifies the RF signal and charges a capacitor. The resulting constant potential is connected voltage divider circuit and is read by a multimeter. The voltages from the pickup and this circuit can then be compared and a calibration factor for the pickup voltage to the voltage on the dee can be extracted. It was found that  $V_{dees} = 0.333988 V/mV_{pp} \cdot V_{pickup}$  at a frequency of 5.831 MHz, so all readings from the pickup could be multiplied to determine the voltage between the dees.

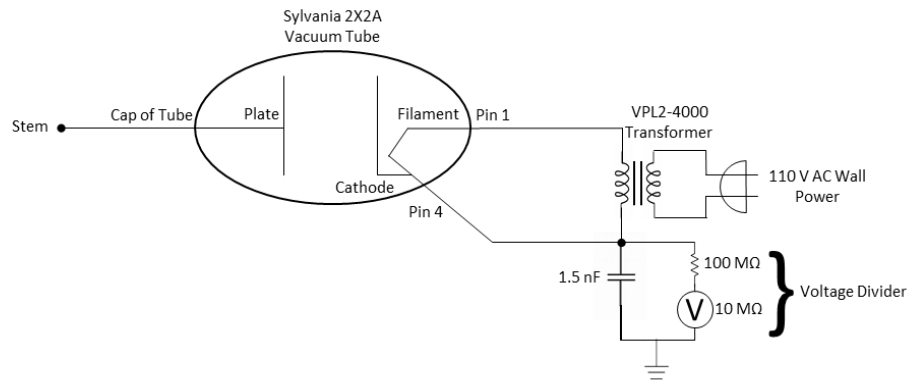


Figure 14. A diagram showing the calibration circuit for the voltage pickup. The voltmeter reads  $\frac{1}{11}$  the total voltage that enters the voltage divider due to the size of the resistors.

### 3.8 Magnet

The magnet used in the Houghton College cyclotron is a GMW Associates 3473-70 that has 15 cm diameter flat pole faces. With a PowerTen R62B-450 magnet supply, this magnet can generate a maximum field of 1.13 T. The magnet is cooled using 0.5 gal/min by a Haskris Co. A5H water chiller that cools water to 10 °C. The magnetic field generated by the magnet is

measured using a TEL-Atomic Inc SMS 102 smart magnetic sensor with its probe placed in a groove of the upper chamber lid.

### 3.9 Vacuum System

The vacuum system consists of an Alcatel model 2012A forepump and a Pfizer Balzers TPU 062 turbopump, controlled by a Pfeiffer TCP040. The turbopump is cooled by the same water chiller as the magnet but using 0.1 gal/min of water. Three pressure gauges are used to ensure this system functions properly. A Kurt J. Lesker model KJL-205 millitorr vacuum gauge is placed in the foreline. A Duniway CVG101GA convection thermocouple pressure gauge and Duniway I-100-K ion gauge are attached to the system after the turbopump and controlled by a Stanford Research Systems Model IGC100 ion gauge controller.

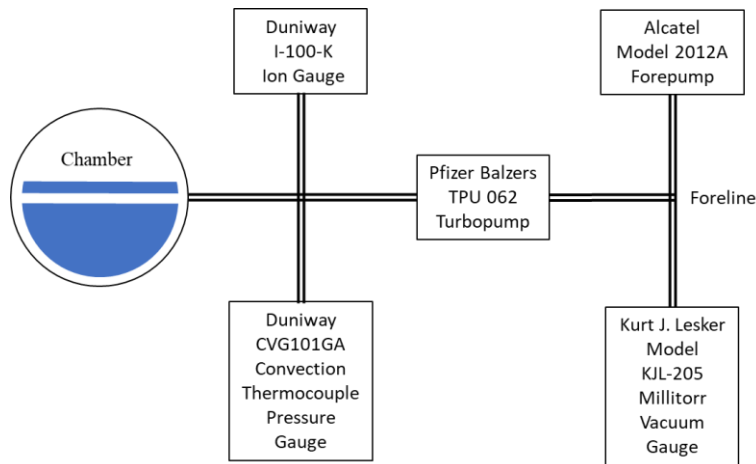


Figure 15. A diagram of the vacuum system of the Houghton College cyclotron.

### 3.10 Target

The target is a piece of copper, of thickness 0.85 mm, bent at a 90-degree angle, held inside the chamber by an MDC K100/BLM-2 motion feedthrough with adjustable length from radii of 88.44 mm to 55.60 mm relative to the center of the chamber. The target is attached to the feedthrough for the Keithley 617 programmable electrometer, which measures the current of the ions striking the target. Behind the target is a ceramic spacer which prevents the current from travelling into the steel arm instead of the electrometer feedthrough. When the beam of accelerated ions strikes the target, electrons may be knocked off the atoms of the target, creating secondary electrons. If the secondary electrons move to the grounded sides

of the chamber, the electrometer will read a higher current than the beam current produced. A 9 V battery is placed between the target and the electrometer to keep the target at a potential of +9 V which attracts secondary electrons back to the target. A new target of thickness 0.53 mm has been machined that has 0.36 mm thick deuterated polyethylene on one side and can be rotated using an MDC BRM-133 feedthrough to cause the plastic or copper to face the beam line. The polyethylene should produce far more reactions than the copper, but the copper allows for checking the beam current.

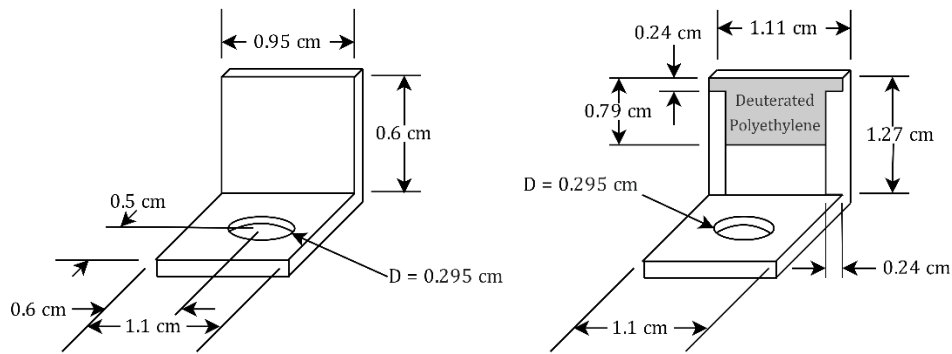


Figure 16. Mechanical drawings of the original copper target and the new copper target with deuterated polyethylene.

### 3.11 Radiation Detector

To detect radiation created by the  $D(d,n)^3\text{He}$  reaction, a Bicron Corp. BC-400 plastic scintillator detector, with a diameter of 5 cm and a length of 15 cm, an Electron Tubes 9266KB04FL phototube operating at a voltage of +1000 V, was used with a Harshaw NB-15X base and scintillator preamplifier. The detector was placed just outside the chamber, about 4 inches from the chamber wall near the window. A plastic scintillator detector detects moving charged particles inside a large piece of plastic. These particles cause the plastic to emit light, which is converted to electrons and multiplied by the photomultiplier tube. The resulting current pulse is proportional to the energy deposited in the detector. Neutrons are best stopped by hydrogen atoms which have the same mass as a neutron and are abundant in plastic. When a neutron strikes a hydrogen nucleus, it can transfer a large portion of the neutron's kinetic energy. The proton moves inside the detector, allowing the detector to register counts for neutrons.

The detector was connected to a DRNL IC 11496 NIM bin containing a Canberra model 3002 HV power supply, ORTEC model 490B amplifier and single channel analyzer (SCA), and ORTEC model 776 counter and timer. All three ORTEC NIM modules receive their power from the NIM bin. The pulses from the detector enter the amp and SCA. In the amp, the detector pulse is shaped and amplified, then the SCA produces a logic pulse each time the amplified input pulse is larger than a selected voltage. This logic signal is then sent to the counter and timer, which counts each pulse and displays the number of pulses in a set window of time. The logic pulses from the SCA are also sent to the National Instruments NI USB-6008 I/O device which also counts them and is read out by the cyclotron control computer.

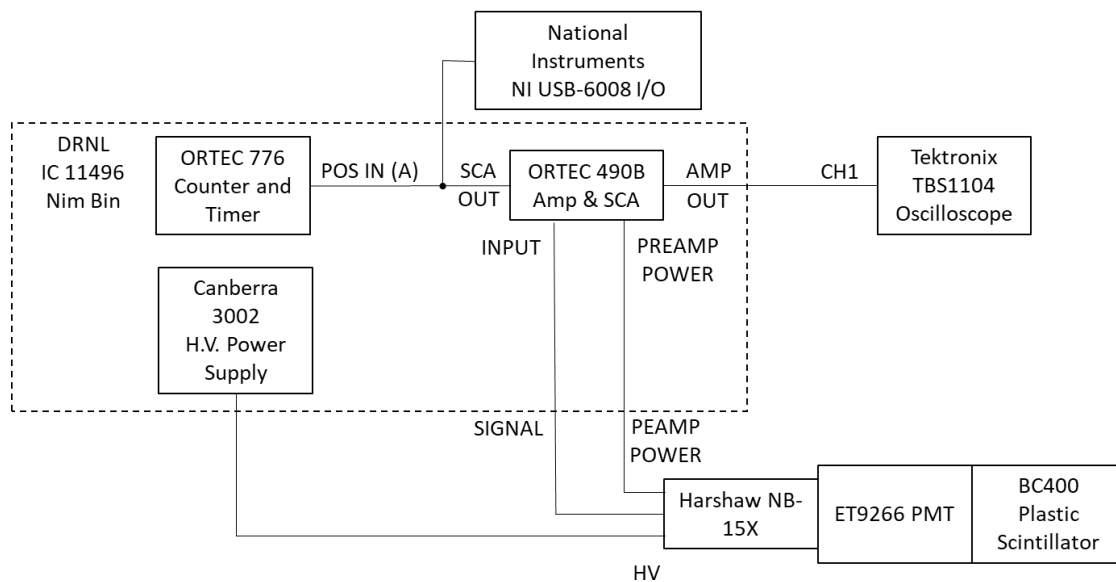


Figure 17. A diagram depicting the circuit for the plastic scintillator detector.

### 3.12 Computer Control

The electrometer, filament power supplies, function generator, magnet power supply, RF oscilloscope, and ion gauge controller are connected via GPIB to a National Instruments GPIB-USB-HS GPIB adaptor. This adaptor is connected by USB to the computer. The teslameter is connected to the computer by RS232. The logic pulses from the SCA enter a National Instruments NI USB-6008 I/O device, which counts the pulses and is read out by

the computer. The information from these systems is collected using a LabVIEW program which saves and plots the measurements and controls the power supplies.

## Chapter 4

### THE D(d,n)<sup>3</sup>He EXPERIMENT

#### 4.1 Overview

The D(d,n)<sup>3</sup>He reaction was selected to be the first nuclear reaction produced using the cyclotron because it requires relatively low energy ions to produce the reaction. This reaction also produces neutrons which can be detected outside the chamber using an internal target and may eventually be used in other experiments. Deuterium-deuterium fusion occurs when two deuterium nuclei collide with sufficient energy to cause the nuclei to fuse together, forming helium-3 and releasing a neutron with 2.45 MeV of kinetic energy. A copper target was used in this experiment. When the beam reached the desired radius, the tip of the protruding copper was struck by the beam, allowing ions to embed themselves in the target or strike ions already embedded in the target.

#### 4.2 Experimental Procedure

Before the cyclotron could accelerate any ions, the function generator had to be set to output the resonance frequency at a reasonable voltage. The frequency was found to be 5.381 MHz with a voltage of 350 mVpp. Next, deuterium gas was let into the chamber from the cylinder by opening the needle valve incrementally while the partial pressure of deuterium in the chamber was measured using the SRS RGA100 residual gas analyzer. This process continued until the partial pressure of deuterium reached  $4 \times 10^{-5}$  Torr. This amount of deuterium could be used to create reactions but would not interfere with accelerating ions.

As deuterium entered cyclotron's chamber and was ionized by the electrons emitted from filament due to thermionic emission, it was accelerated until it reached a radius of 5.54 cm, where it hit the copper target. The first deuterium ions to reach the copper target embedded themselves in the copper, allowing later deuterium ions to collide with the embedded ions, resulting in D(d,n)<sup>3</sup>He fusion. Since the target was made of copper, it was connected to an electrometer in order to measure the current of ions striking the target. This allowed for the optimal magnetic field for accelerating the particles to be determined. To this end, a program

was written in LabVIEW, see Appendix A, to scan the magnet current and to record the resulting magnet field strength and beam current from the teslameter and electrometer, respectively. The predicted magnetic fields and energies of the peaks for deuterium and hydrogen atoms were calculated using Equation (8) and labelled on the measured beam current vs. magnetic field plot, as shown in Figure 18. A peak in beam current for deuterium at 255 mT was selected since it was the largest peak having highest energy. A second scan was then taken with the magnetic field around 255 mT, see Figure 19, in order to find the optimal magnet current was 8.464 A, resulting in a beam current of about 20 nA at an energy of 4.8 keV for ions incident on the target. After this, the cyclotron was powered on with the magnetic field set to this value.

The  $D(d,n)^3He$  reaction ejects a neutron, which can be detected to verify that the reaction has taken place. Neutrons, because they have no charge, easily passed through the chamber wall. A plastic scintillator detector was placed outside the chamber to detect neutrons produced. The cyclotron was powered on, and 20 nA of 4.8 keV deuterons were accelerated into the copper target for 50 min. During the next 50 min, plastic scintillator pulses were counted while deuterons continued striking the target. The background was counted with the filament turned off, meaning the deuterons were not ionized so they could not be accelerated into the target, for 50 min.

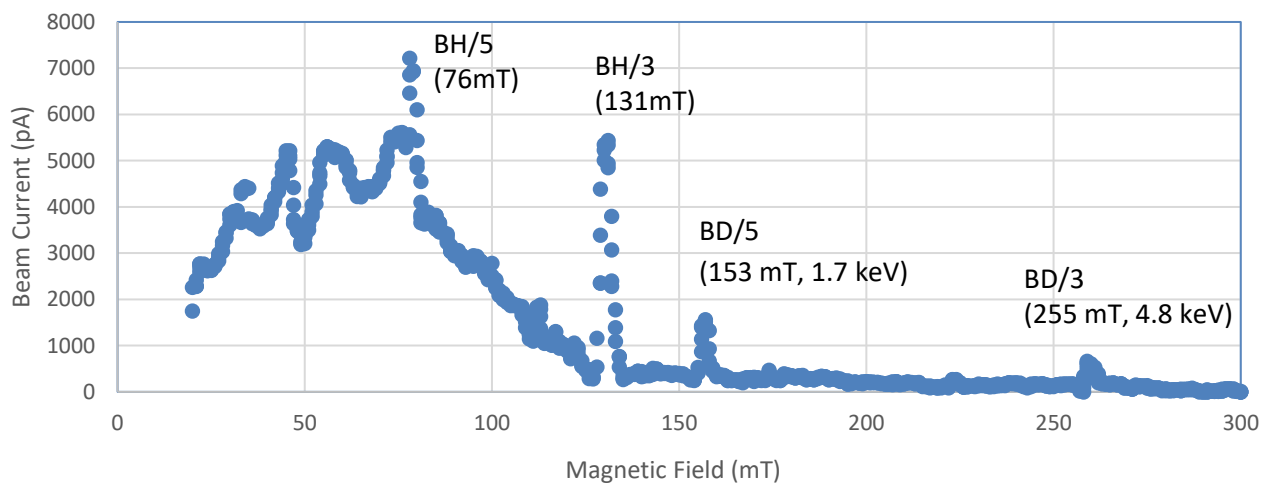


Figure 18. Measured beam current as a function of the magnetic field for deuterium gas. The BD/5 and BD/3 peaks are the peaks for deuterium ions. The BD/3 peak was selected because it had the highest energy.

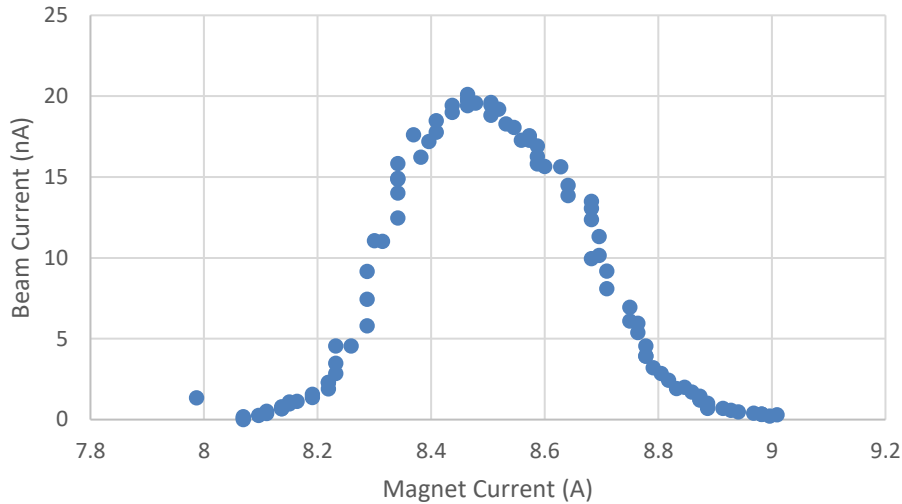


Figure 19. Beam current as a function of magnet current near 255 mT. The peak is at a magnetic current of 8.464 A, corresponding to a beam current of about 20 nA.

### 4.3 Results

While increased radiation was produced, a Thermo Eberline NRD helium-3 neutron detector with attached dosimeter was used to ensure that the radiation level was safe, and it never exceeded 2.5  $\mu$ Rem during the experiment. Even so, since the cyclotron is controlled remotely, no one was in the same room as the cyclotron while it was emitting radiation. The number of counts with the filament on was 176286 counts and the background was 168373 counts. Thus, the data set with the beam powered on accrued 7913 more counts than the background data set, yielding  $7913 \pm 587$  counts from deuterons striking the target in 50 min. Using the low estimate for the number of neutrons in found using Equation (10), that less than 2.24 reactions would occur in an hour, the experiment produced a surprisingly large number of reactions. This could mean that the reaction in the chamber was not deuterium-deuterium fusion and produced large numbers of gamma rays that were detected. It could also mean that the cross section used to create an estimate for the number of reactions was not correct, a possibility supported by Figure 8 and Figure 9, where the data disagrees at low cross sections. Further experiments will be necessary to determine the cause of the high counts.

## *Chapter 5*

### CONCLUSIONS

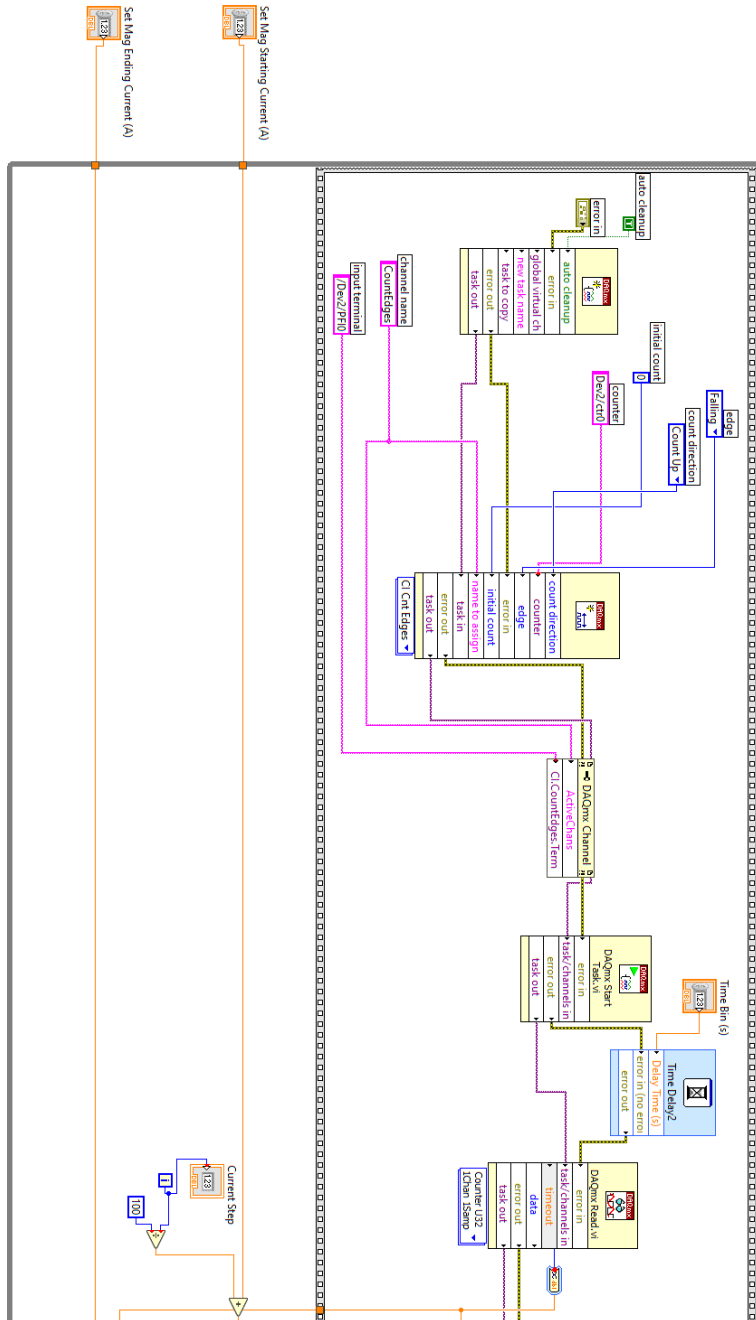
Although this measurement was consistent with deuterium-deuterium fusion having occurred, the plan is to run this experiment again with modifications to make sure this reaction was produced. A helium-3 neutron detector will eliminate possible misidentification of gamma rays or x-rays. An important factor that will help ensure neutrons are produced is to increase the yield. The new target with deuterated polyethylene will be used, that should increase the number of reactions that occur by increasing the number of available target nuclei. Accelerating deuterons to higher energies would also increase the yield. The Houghton College cyclotron has previously accelerated ions to 160 keV, compared to the 4.8 keV achieved in this experiment. Higher energies would increase the likelihood of reactions occurring, as was shown on the cross-section plot. By re-tuning the inductors in the dee power circuit, resonance will be made to occur at stronger magnetic fields, increasing the energy of the accelerated ions.

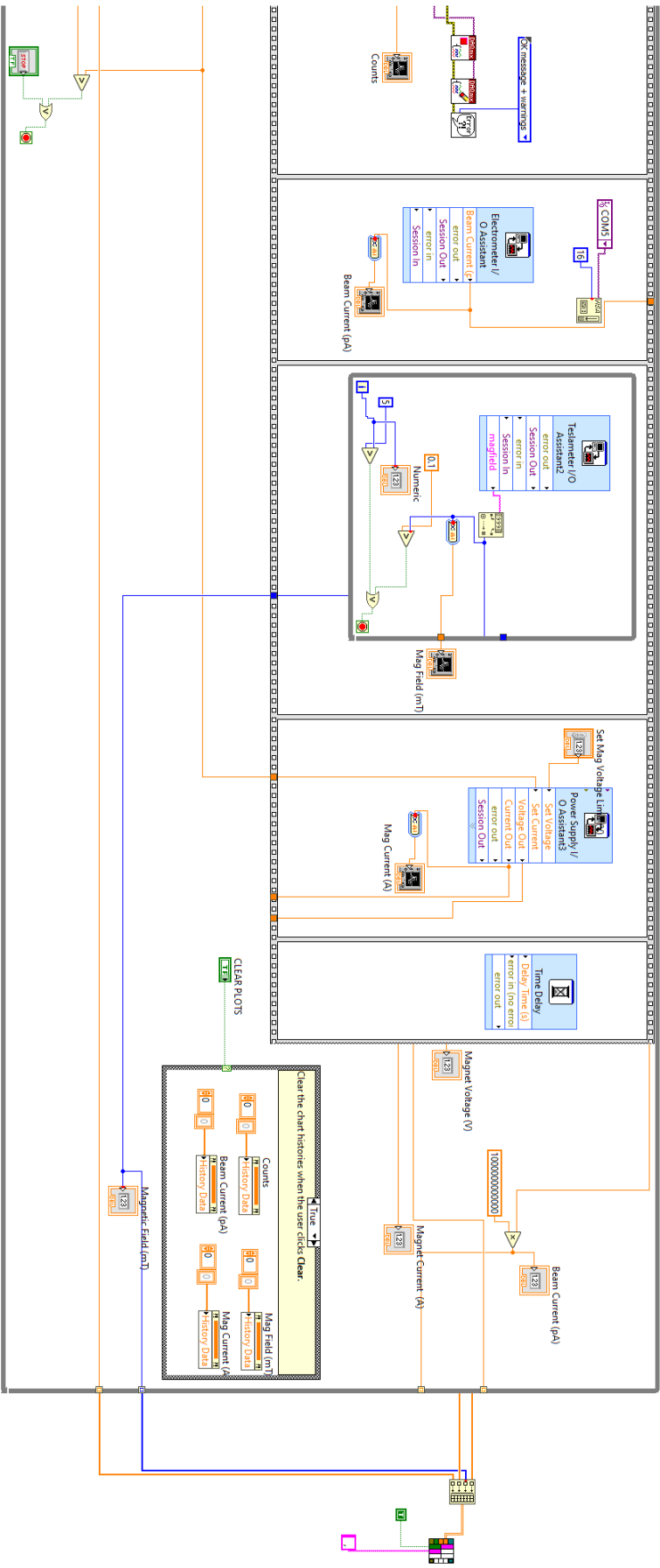
The Houghton College cyclotron is limited in the energies it can produce because it uses weak focusing. In the long term, using strong focusing instead of weak focusing is being investigated. With strong focusing, the maximum achievable energy could reach 900 keV. A Mathematica code has been written that simulates the magnetic field from the pole tips and the movement of ions. We will use the code to help design new pole tips that take advantage of strong focusing.

# Appendix A

## LABVIEW CODE

The LabVIEW program saves and plots measurements and controls the power supplies for the Houghton College cyclotron.





## Appendix B

### SMATH CROSS SECTION CALCULATION

This is the SMath calculation used to estimate the number of neutrons produced in the cyclotron during the D(d,n)<sup>3</sup>He experiment.

## DD neutron production estimate

### Units

$$eV := 1.6021 \cdot 10^{-19} \text{ J}$$

$$keV := 1000 \cdot eV$$

$$MeV := 1000 \cdot keV$$

$$mb := \frac{\text{barn}}{1000}$$

$$CD2\_dens := 0.975 \frac{\text{g}}{\text{cm}^3}$$

density of polyethylene

$$CD2\_d\_num\_dens := \frac{CD2\_dens \cdot 2}{12 \frac{\text{g}}{\text{mol}} + 2 \frac{\text{g}}{\text{mol}} + 2 \frac{\text{g}}{\text{mol}}} N_A = 7.3395 \cdot 10^{22} \frac{1}{\text{cm}^3}$$

deuterons/cm<sup>3</sup> for 100% deuterated polyethylene

$$i := 20 \text{ nA}$$

$$A := 1 \text{ cm}^2$$

$$t := 1.11 \text{ hr}$$

$$N := \frac{i}{e} \cdot t = 4.9882 \cdot 10^{14}$$

### For ions stuck in copper

$$\text{DD cross section at 10 keV} \quad \sigma := 0.01 \cdot mb = 1 \cdot 10^{-33} \text{ m}^2 \quad Y := \sigma \cdot \frac{i}{e} \cdot \frac{N}{A} = 2.2416 \frac{1}{\text{hr}}$$

$$\text{DD cross section at 100 keV} \quad \sigma := 0.015 \text{ barn} = 1.5 \cdot 10^{-30} \text{ m}^2 \quad Y := \sigma \cdot \frac{i}{e} \cdot \frac{N}{A} = 3362.4708 \frac{1}{\text{hr}}$$

### for polyethylene

$$\text{Range of 10 keV} = 2000 \text{ \AA} \quad 2000 \text{ \AA} = 0.2 \text{ \mu m}$$

$$\text{Range of 100 keV} = 1.2 \text{ \mu m}$$

$$\begin{aligned} \text{DD cross section at 10 keV} \quad \sigma &:= 0.01 \cdot mb = 1 \cdot 10^{-33} \text{ m}^2 \\ Y &:= \sigma \cdot \frac{i}{e} \cdot CD2\_d\_num\_dens \cdot 0.2 \text{ \mu m} = 6596.5631 \frac{1}{\text{hr}} \end{aligned}$$

$$\begin{aligned} \text{DD cross section at 100 keV} \quad \sigma &:= 0.015 \text{ barn} = 1.5 \cdot 10^{-30} \text{ m}^2 \\ Y &:= \sigma \cdot \frac{i}{e} \cdot CD2\_d\_num\_dens \cdot 1.2 \text{ \mu m} = 5.9369 \cdot 10^7 \frac{1}{\text{hr}} \end{aligned}$$

## References

- 
- [1] E. Rutherford, *Proc. Roy. Soc. (London)* **117**, 300 (1927).
- [2] G. Ising, *Ark. Math. Astron. Phys.* **18**, 45 (1925).
- [3] R. Wideröe, *Arch. Elektrotech.* **21**, 387 (1928).
- [4] M. S. Livingston and J. P. Blewett, *Particle Accelerators*, (McGraw-Hill Book Company, Inc., New York, 1962), p. 140-141, 144, 148-149.
- [5] E. O. Lawrence and N. E. Edelfsen, *Science* **72**, 376 (1930).
- [6] M. S. Livingston, Ph.D. thesis, University of California, 1931.
- [7] M. S. Livingston, *Journal of Applied Physics* **15**, 2, (1944).
- [8] E. M. McMillan, *Physics Review* **68**, 143 (1945).
- [9] W. M. Brobeck, E. O. Lawrence, K. R. Makenzie, E. M. McMillan, R. Serber, D. C. Sewell, K. M. Simpson and R. L. Thornton, *Physics Review* **71**, 449 (1947).
- [10] G. Schatz, in *Proceedings of the 9th International Conference on Cyclotrons and their Applications, Caen, 1982*, edited by G. Gendreau, p. 661.
- [11] G. Dutto, in *Proceedings of the 13th International Conference on Cyclotrons and their Applications, Vancouver, 1993*, edited by G. Dutto and M. K. Craddock, p. 138.
- [12] R. C. York, H. G. Blosser, T. L. Grimm, F. Marti, J. Vincent, X. Wu and A. Zeller, in *Proceedings of the 15th International Conference on Cyclotrons and their Applications, Bristol, 1999*, edited by E. Baron and M. Lieuvain, p. 687.
- [13] B. V. Siegel and R. C. Sinnot, *Physics Today* **1**, 10 (1948).
- [14] K. J. Bertsche, C. A. Karadi and R. A. Muller, *Nuclear Instruments & Methods in Physics Research* **A301**, 358 (1991).
- [15] T. Feder, *Physics Today* **57**, 30 (2004).
- [16] Leslie Dewan, B.S. thesis, Massachusetts Institute of Technology, 2007.
- [17] H. Baumgartner, in *Proceedings of the 20th International Conference on Cyclotrons and their Applications, Vancouver, 2013*, edited by J. Thomson and V. R. W. Schaa, p. 302.
- [18] C. Wolf, M. Frank, E. Held, *Proceedings of the 20th International Conference on Cyclotrons and their Applications, Vancouver, 2013*, edited by J. Thomson and V. R. W. Schaa, p. 296.
- [19] M. H. G. Prechtel and C. M. Wolf, *Das Lehr-Zyklotron COLUMBUS*, (Springer Spektrum, Wiesbaden, 2020).
- [20] B. King, B.S. thesis, Houghton College, 2003.
- [21] M. Cressman, B.S. thesis, Houghton College, 2006.
- [22] D. Haas, B.S. thesis, Houghton College, 2009.
- [23] S. Morrow, B.S. thesis, Houghton College, 2015.
- [24] M. Yuly, *Proceedings of the 20th International Conference on Cyclotrons and their Applications, Vancouver, 2013*, edited by J. Thomson and V. R. W. Schaa, p. 286.
- [25] National Nuclear Data Center <https://www.nndc.bnl.gov/>.
- [26] W. R. Arnold, J. A. Phillips, G. A. Sawyer, E. J. Stovall Jr, and J. L. Tuck, *Physical Review* **93**, 483 (1954); R. E. Brown and N. Jarmie, *Physical Review C* **41**, 1391 (1990); A. S. Belov, V. E. Kusik, and Yu. V. Ryabov, *Nuovo Cimento* **A103**, 1647 (1990); V. M. Bystritsky, V. V. Gerasimov, A. R. Krylov, S. S. Parzhitski, P. S. Anan'in, G. N. Dudkin, V. L. Kaminskii, B. A.

---

Nechaev, V. M. Padalko, A. V. Petrov, G. A. Mesyats, M. Filipovicz, J. Wozniak, and V. M. Bystritskii, *European Physical Journal A* **36**, 151 (2008).